DROP DEPOSITION AND LOW-SPEED IMPACT ON FLAT, CURVED AND MICROFINNED SOLID SURFACES: COMPARISON BETWEEN SIMULATIONS, MODELS AND EXPERIMENTS

Manfredo GUILIZZONI[1,C]

[1]Department of Energy, Politecnico di Milano - Via Lambruschini 4, 20156 Milan
[C]Corresponding author: manfredo.guilizzoni@polimi.it

ABSTRACT
The two-phase and multiphase incompressible solvers of the OpenFOAM® CFD package were used to simulate the shape, gentle deposition and low-speed impact of water drops on solid surfaces characterized by means of the contact angle. Smooth flat and curved surfaces and microfinned surfaces were used to benchmark such solvers by comparison with numerically-integrated analytical results, models and experimental results. The simulation were performed on single personal computers to verify what can be obtained with a conventional hardware, without using a cluster. The observed performances are satisfactory even if some problems were encountered.

INTRODUCTION

Numerical simulation is more and more used in many engineering fields and it has reached a high level of reliability for the analysis of complex problems, which up to a few years ago could only be investigated experimentally or by means of very simplified models. Nevertheless, it remains a "dangerous" instrument due to the ill-reposed trust it may give if incorrectly used [1] and there is still a need for further benchmark of simulation results, particularly in those field where simulation is "younger" or more difficult. Computational fluid dynamics (CFD) of multiphase flows is certainly one of the latter cases. Moreover, during the last years many studies were devoted to the development of new materials and surfaces with special characteristics, among which one of the most interesting features is hydrophobicity. Wettability analyses thus gained renewed importance. For the present work, comparisons between numerical, experimental and analytical results was therefore performed for some cases in the fields of drop deposition and low-speed impact onto solid surfaces, to verify the performances of the *interFoam* and *multiphaseInterFoam* solvers of the OpenFOAM® CFD package [2]. The code structure, implemented models and open source nature of OpenFOAM® makes it a very interesting and promising tool, and good results were obtained with it for various multiphase fluid dynamics problems [3–15]. They are mainly related to highly dynamic cases (e.g. drop impact onto liquid [3–8] and solid [9] surfaces), while very few studies [10] are devoted to static or low-speed scenarios. In this work some situations of the latter kind were investigated, with main focus on sessile and gently deposed drop. Smooth flat and curved surfaces and microfin surfaces were tested, by means of axisymmetric and 3D simulations run on structured meshes. A drop-onto-drop impact at 1.4 m/s was also tested.

NUMERICAL PROCEDURE AND INVESTIGATED CASES

Table 1 shows the details of the investigated cases. The *interFoam* solver of the OpenFOAM® open source CFD toolbox [2] was chosen because of its very promising characteristics (e.g. automatic interface tracking and mass conservation) [16–18] and because successful examples of use of *interFoam* in the fields of drop splashing and impact are reported in literature [3–9]. *interFoam* is a two-phase finite volume solver which uses a Volume of Fluid (VOF) [19] approach modified with the introduction of an additional term in the volume fraction equation, to obtain interface compression by means of a tunable parameter. The continuum surface force (CSF) model [20] is used to include surface tension at the interface. A detailed descriptions of *interFoam* and of the underlying models can be found in [3, 4, 16–18, 21]. For one of the simulations, the *multiphaseInterFoam* solver [15, 22] - which is an extension of *interFoam* - was also used. OpenFOAM® versions 1.7.1 and 2.1.x gave practically identical results for the performed simulations. No modifications were done to the solver and the discretization schemes and settings from the official *damBreak* tutorial case were used. The domain was modelled and meshed with the *blockMesh* OpenFOAM® utility. Non-flat domain floors (curved or microfinned) were modelled using Matlab® and in most cases the *snappyHexMesh* OpenFOAM® utility. Purely structured hexahedral meshes were created, apart from the cases where *snappyHexMesh* was used, as the snap of near-boundary cells to the boundary surface results in non-structured mesh regions. In one case (deposition on a microfin surface, case 3b) a home-made pre-processing utility for *blockMesh* was also tested. Domain and mesh dimensions are given in Tab. 1. In all cases the domain is opened on the top, where "open boundary" conditions were implemented. On the sides of the domain either symmetry conditions (axis or plane) or "zero gradient" wall boundary conditions were set for all variables. On the floor of the domain, which is the surface touched by the drops, boundary conditions implementing "constant contact angle" were set. As a first test, contact angle hysteresis (which could have been implemented using the built-in dynamical contact angle boundary condition or more sophisticated models [23, 24]) was neglected. Water drops at ambient temperature (20 °C) were used, with air as a surrounding medium. Both fuids were assumed Newtonian and incompressible and the flow laminar. Water regions were initialized using the *setFields* and *funkySetFields* OpenFOAM® utilities. The solver is let free to adapt the time step to keep the Courant number under 0.5. Such requirement is the limit for 2D simulations using the scheme implemented in OpenFOAM® and should be

reduced to under 0.3 for 3D cases [17, 18]. The problem is addressed by the introduction of some volume fraction sub-cycles. For some cases much lower Courant numbers may be a better solution, particularly to reduce spurious velocities, but this would imply very small time steps and consequently extremely long simulations. As for Newtonian fluids the viscosities of the phases do not intervene in the drop final equilibrium shape, for cases where the latter was the only interest they were increased 100 times with respect to their real values. This partially smooths out the oscillations and speeds-up the convergence to the final shape. For the same cases, the simulations were run until the drop shape visually did not change any more and the maximum speed within the domain was reduced under 0.01 m/s - a purely arbitrary choice, with no further analysis about real or spurious velocities apart from qualitative meaningfulness of the results (Figs. 1, 2). Concerning the used hardware, simulations were performed on a notebook PC with a Intel Core i7-740QM CPU (4 cores @ 1.73 GHz, 8 threads) with 6 GB RAM and on a desktop PC with a Intel Core i7-990X CPU (6 cores @ 3.46 GHz, 12 threads) with 24 GB RAM, both with Ubuntu Linux as the operating system.

Case	**Surface type**	**Drop speed [m/s]**	**2D / 3D simulation**	**Domain [mm] and number of cells**
Wetting drop	Smooth, flat	Sessile	2D axisym.	5x5, 62500, 250000, 1000000
Nonwetting drop	Smooth, flat	Sessile	2D axisym.	5x5, 62500
Drops on curved surface	Smooth, curved	Sessile	3D	5x11x10, 2140842
Drop on microfin surface	Microfin	Gently deposed (very low speed impact)	3D	case 1: 4x4x5, 2118150; case 2 and 3a: 10x5x4.23, 2911000; case 3b: 10x5x4.23, 3125000
Drop-onto-drop impact	Smooth, flat	1.4	2D axisym.	5x5, 62500

Table 1: Details of the investigated cases.

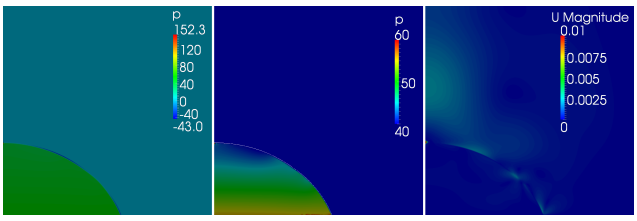

Figure 1: Wetting drop: pressure and velocity magnitude at "equilibrium".

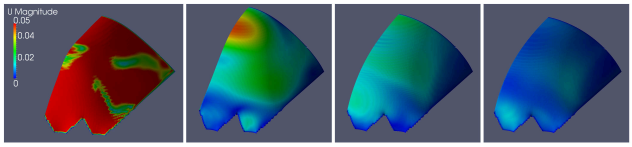

Figure 2: Deposition on the microfin brass surface: reduction of the velocities towards equilibrium (time = 100:10:130 ms).

EXPERIMENTAL SET-UP

The set-up available at the Multiphase Fluid dynamics Laboratory of the Department of Energy, Politecnico di Milano was used for the experimental validation of the results. It is located on an anti-vibrating optical bench (Newport, SA Series, 1.2 x 0.80 m) with a carrying structure in aluminium alloy. A high precision metering pump (Cole-Parmer Instrument Company, model AD74900) completed by suitable syringes and needles (Hamilton) allows to generate microlitre drops of controlled volume. The surfaces under investigation can be characterized, in terms of profile and roughness, by means of a "surface analyzer" (SM Sistemi di Misura s.r.l., model RT80). A 800 W lamp equipped with a diffuser provides the lighting necessary to the photographic and video acquisitions. Still images can be taken using a SLR digital camera Nikon D90 with a AFS 60mm F2.8 Macro lens, while a Canon DM-XM2 videocamera and a Nikon AW100 compact camera can be used to capture videos at 25, 120 and 240 fps. Detailed description of the experimental procedure for image processing, contact angle measurement and drop shape analysis can be found in [25] for flat and curved surfaces and in [26] for microfin surfaces.

WETTING DROP ON A FLAT SURFACE

The first investigated case was the sessile drop on a hydrophilic (contact angle 70°) ideal (chemically omogeneous, smooth, flat) solid surface. A 2D axisymmetric simulation was performed. The drop was initialized as a cylinder (height = 2 mm, diameter = 4 mm) using the *setFields* OpenFOAM® utility and let evolve towards its final equilibrium shape. In the given conditions, the latter may be described by the Laplace-Young equation which for the sessile drop case reads (ΔP_{apex} being the pressure jump at the drop apex, y axis centered in the drop apex and with downward direction):

$$\Delta P_{apex} + \left(\rho_{drop} - \rho_{\substack{surrounding\\fluid}}\right) g y = = \sigma_{LV}\left(\frac{1}{R_1} + \frac{1}{R_2}\right) \quad (1)$$

or in arc length coordinates (s,ϕ) [27]:

$$\frac{d\phi}{ds} = \frac{2}{R_{apex}} + \frac{\left(\rho_{drop} - \rho_{\substack{surrounding\\fluid}}\right) g}{\sigma_{LV}} y - \frac{sin\phi}{x} \quad (2)$$

where R_{apex} is the curvature radius at the drop apex.

Equation 2 may be easily integrated numerically so that comparison between such result and the output of numerical simulations can be performed. The latter should trivially reproduce the correct contact angle, which is set as a boundary condition, but also the Laplacian drop profile. As the method implemented in OpenFOAM® is a volume method and the shape and position of the interface is not explicitly tracked, such check is a validation of the model, to see if it is able to reproduce correct interface shapes. As already told, the simulations were run until the drop shape visually did not change any longer and the maximum speed within the domain reduced under 0.01 m/s. At that point, a cross-section of the calculated drop shape was extracted by the ParaView® postprocessor and saved as an image. For all the cases described in the paper, the drop surface was extracted as the isosurface for volume fraction equal to 0.5. No significant difference would in any case appear if other values in the range 0.1-0.9 should have been used. Cross-section of such isosurface were then extracted when needed, as in this case. The procedure for drop shape analyis described in [25, 26, 28] was then applied using such image instead of an experimental side-view picture of a drop. Figure 3 shows the results of the comparison. As it can be seen, the agreement both in the contact angle and in the drop profile is very good. This first investigated case will serve also as a basis for a following one, where another drop will be let fall on the sessile one analysed here.

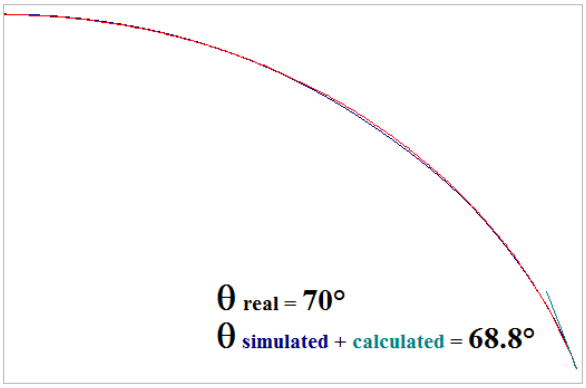

Figure 3: Comparison between the numerical and "analytical" (numerical integration of the Laplace-Young equation) results for the shape of a water drop on a hydrophilic surface.

Figure 4 shows the mesh dependence of the simulation results: it is evident how the drop evolution from the initial cylindrical shape to the final equilibrium shape is heavily dependent on the mesh at the beginning, while the final shape is correctly reproduced with all the three meshes.

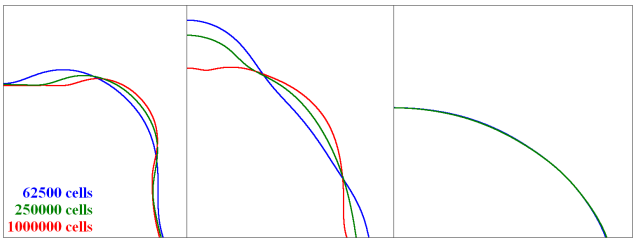

Figure 4: Wetting drop: mesh [in]dependence of the results (time = 10 ms, 20 ms, 200 ms).

NONWETTING DROP ON A FLAT SURFACE

The same kind of analysis was then performed for a drop on a hydrophobic surface (Fig. 5) The contact angle was modified into 120°, while all the other settings were left unaltered. Many side views of the numerical drop profile were extracted at different zoom levels, to investigate also the effect of the image resolution on the procedure for drop shape analysis. As it can be seen in Fig. 6, the latter as almost no influence and the agreement between *interFoam* results and the Laplacian drop profile is very good in this case too.

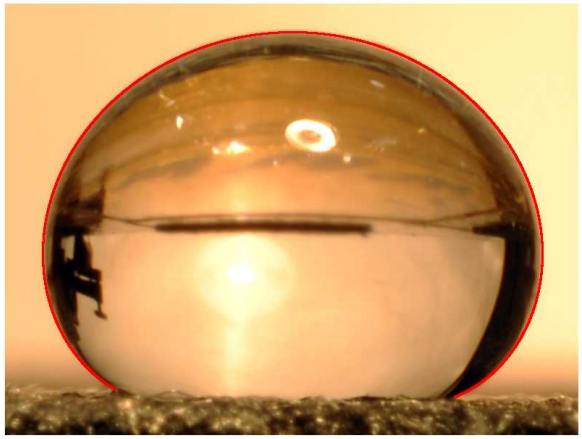

Figure 5: Water drop on a hydrophobic surface. The drop contour fitted with the procedure described in [25] is evidenced, showing the very good agreement between the Laplacian and the real drop profiles.

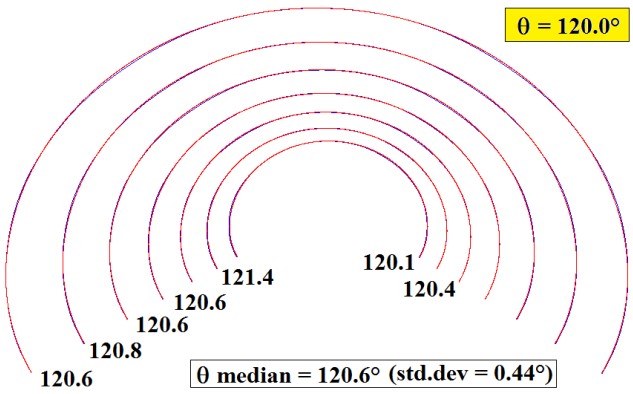

Figure 6: Comparison between the numerical and "analytical" (numerical integration of the Laplace-Young equation) results for the shape of a water drop on a hydrophobic surface and contact angle determination using images with different resolutions, to investigate the effect of such parameter on the measurement.

The ability of *interFoam* to correctly reproduce drop shapes (both in wetting and nonwetting conditions) may allow its use for improved VOF simulations of cases where the drop shape has been up to now considered as spherical or commercial solvers have been used (e.g. simulation of dropwise cooling [29–31], drop growth and detachment in the channels of fuel cells [32–34]).

WETTING DROPS ON A CURVED SURFACE

In a previous paper [25], a procedure to determine the static contact angle from measurements on curved surfaces was proposed. On a curved surface, if the drop is not perfectly symmetric with respect to the curvature (as it is in [35]) the contact angle is still a static as-placed one [36], but at each point of the contact line a different component of "recession" or "advancement" can be hypothesized [37] (Fig. 7), so that a different contact angle in the spectrum between the minimum receding and the maximum advancing contact angles is actually measured. Therefore, a new approach was proposed: the angle between the tangent to the drop profile and the horizontal ("drop angle" in the following) is plotted as a function of the angle between the tangent to the base profile and the horizontal ("base angle" in the following). The angles are measured from $-\pi$ to $+\pi$ along with the scheme shown in Fig. 8. Such function shows a fair linear trend and a linear fitting can be calculated. The intercept of the fitting is the value of the drop angle in correspondence of a horizontal baseline (base angle = 0^o). The linear fitting implicitly keeps in account the "advancing" and "receding" contributions to the drop angles due to the baseline inclination, contributions which are zero when the baseline is horizontal. Therefore the cited intercept is an estimate for the "equilibrium" contact angle of an "as placed" drop on a flat surface. From that, the maximum advancing, minimum receding and equilibrium contact angles can be estimated following the approach described in [36].

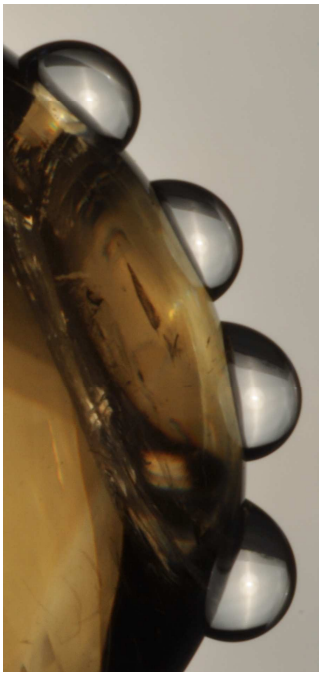

Figure 7: Drops on a curved surface: effect of the surface curvature and inclination.

For the present paper, the described procedure was applied to numerically simulated drops on curved surfaces. Such surfaces were created and converted into a STL file using Matlab® and they were introduced as the bottom boundary of the domain using the *snappyHexMesh* OpenFOAM® utility. Boundary conditions of slight hydrophobicity (static contact angle 100^o) were set on such surfaces. The drops

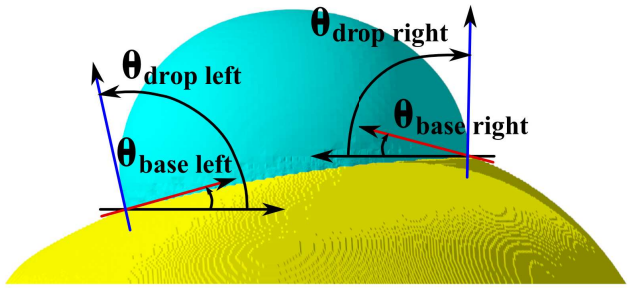

Figure 8: Sketch of the measured angles for contact angle determination on a curved surface.

were initialised as spheres intersecting the curved domain floor using the *funkySetFields* OpenFOAM® utility and let evolve towards their equilibrium shape. Then, base and drops contours were extracted as before from cross-sections of the results using ParaView®. Smoothing splines were fitted to each contour and tangents to the resulting curves were calculated at the contact points. Fig. 9 and 10 show an example of results. The agreement is good and this is a confirmation of the validity both of the simulations and of the procedure.

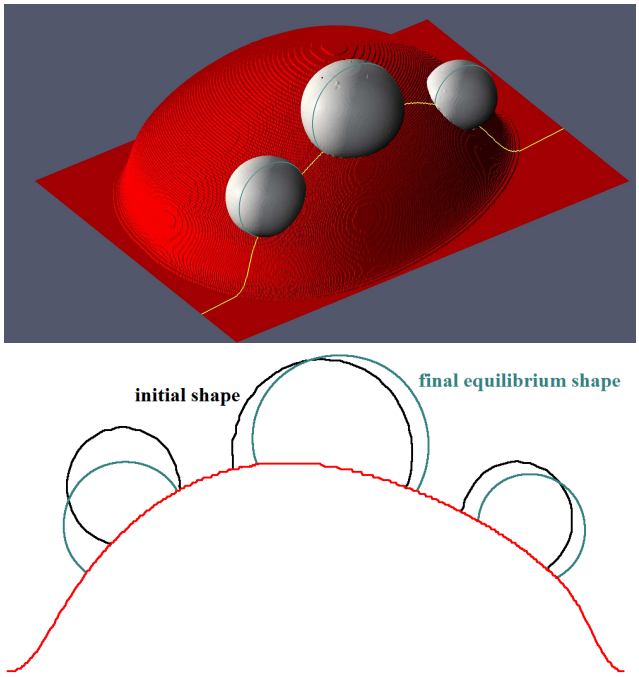

Figure 9: Drops on curved surfaces: 3D view of the equilibrium shape and cross-sections of the initial and final shapes.

DROP DEPOSITION ON A MICROFIN SURFACE

At the Department of Energy, Politecnico di Milano has been active for some years now a research program about drop interaction with microfin surfaces, both from the adiabatic point of view (drop deposition and impact, drop shape, contact angles - Fig. 11) and from the thermal point of view (evaporative dropwise cooling) [26, 38]. Comparisons were therefore performed between numerical simulations and experimental data for drop deposition and drop shape on surfaces with microfins having triangular section. Three

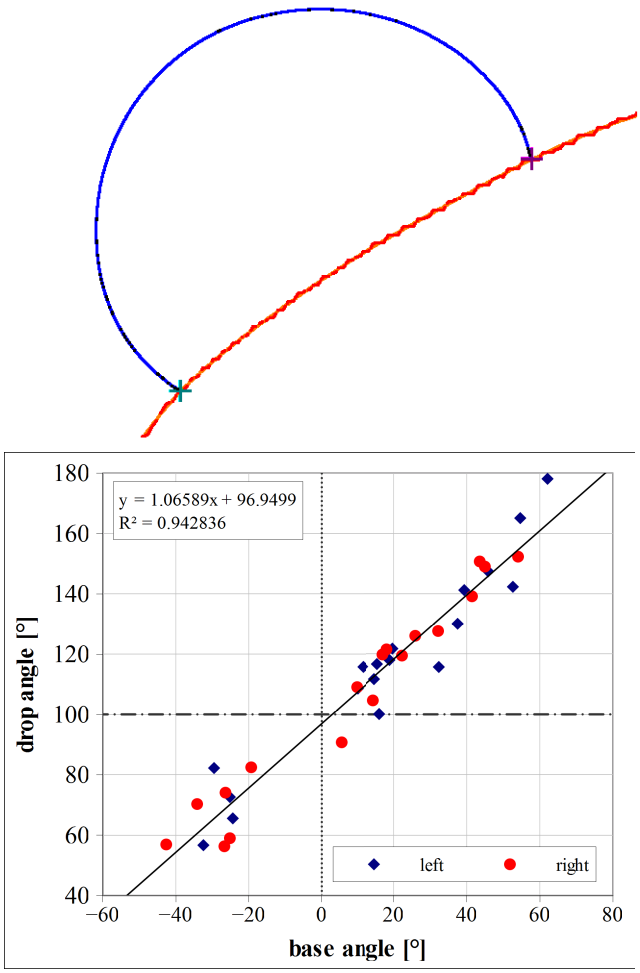

Figure 10: Drops on curved surfaces: contact angle measurement using the procedure described in [25].

cases were simulated: the deposition of a $85 \cdot 10^{-9}$ m^3 water drop onto an aluminium microfin surface characterized by microfin height H = 250 µm, base B = 500 µm, spacing S = 880 µm (case 1), and the deposition of a $85 \cdot 10^{-9}$ m^3 (case 2) and a $80 \cdot 10^{-9}$ m^3 (case 3 a and b) water drops onto a brass microfin surface characterized by microfin height H = 400 µm, base B = 865 µm, spacing S = 1250 µm. For cases 1, 2 and 3a the surface was modelled and converted into a STL file using Matlab® and then introduced as the bottom boundary of the domain using the *snappyHexMesh* OpenFOAM® utility. For the third case, a home-made pre-processing Matlab® file was also tested. It creates a *blockMeshDict* file readable by the *blockMesh* OpenFOAM® starting from two matrixes containing the heights of the "floor" and the "ceiling" of the domain (case 3b). Figure 12 shows some details of the geometry and mesh for the different cases.

The drop was initialized as a sphere with the lower point at $5 \cdot 10^{-4}$ m over the base surface, then it was let fall due to gravity and evolve towards the static equilibrium shape. Such relaxation time is quite long if compared with the time step imposed to respect the Courant number limits: setting real viscosities, it is of the order of 0.3-0.4 s to macroscopically reach the final shape (despite oscillations are still present); it becomes shorter and with dampened oscillations if increased

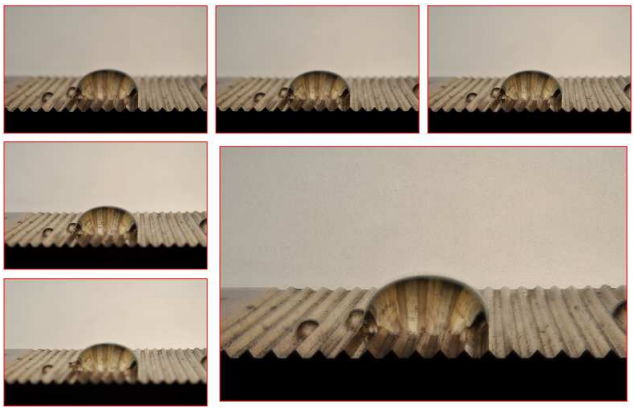

Figure 11: Deposition on the brass 400 µm microfin surface, 85 µl water drop: experimental results with DOF enhancement by image blending, in order to focus both the drop and the surface sample.

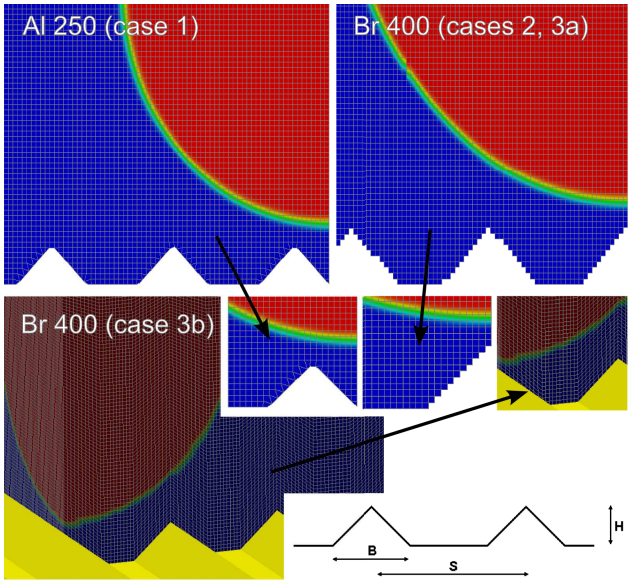

Figure 12: Drop deposition on microfin surfaces: details of the geometry and meshes for the three investigated cases.

viscosities are used. The consequence is that the simulation were extremely time consuming (up to 28 days for case *3b*).

Figures 13, 14, 15 show some results from the simulations, while Figs. 16, 17 show some image sequences (to be observed row-wise) extracted from experimental video acquisitions at 240 fps. They were adjusted in brightness and contrast to improve their visibility. The case in analysis is the gentle deposition of a drop of water on the brass 400 µm microfin surface. Despite the very low resolution (320x240 px) of the experimental images, they allow to observe the good agreement with the numerical results from the qualitative point of view and in terms of time duration of the deposition transient. Figure 18 shows an analogous image sequence for a low-speed drop impact, where the same features highlighted in [39] (e.g. ridges, aligned drop front) can be recognized.

Concerning the final equilibrium condition, the drop shape and dimensions were compared with experimental results and models [40]. Starting from the latter, Fig. 19 shows the results of the comparison of the simulated contact profile (case 3a) with the equation by Chen *et al.* [40]. As the

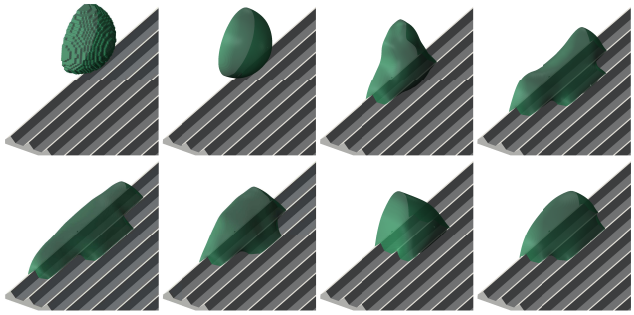

Figure 13: Drop deposition on the aluminium 250 μm microfin surface: 3D view of the numerical drop shape evolution (drop volume 85 · 10^{-9} m^3, time = 0:14:98 ms).

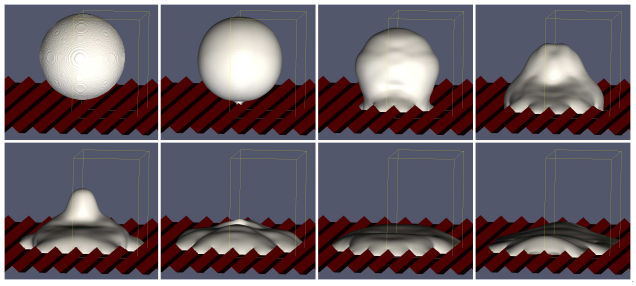

Figure 14: Drop deposition on the brass 400 μm microfin surface: 3D view of the numerical drop shape evolution (drop volume 85 · 10^{-9} m^3, time = 0:8:48 ms).

drop dimensions are an input for the model, the true subject of the comparison is the projected shape. The agreement is satisfactory, particularly if considering that the model was developed for smaller grooves, which impose a much smaller distortion to the drop.

On the contrary, the agreement is not good when the cross-microfin section is considered (Fig. 20). The simulated drops cover the same number of grooves of the real ones, but the 85 μl drop on the brass surface is much lower than the real one. For case 3a, part of the fault is of the modelling of the microfin surface: creating it as a jagged surface forces the contact angle to be imposed on a horizontal or vertical surface, while in reality the contact line is along a oblique surfaces. Case 3b was run specifically to verify this aspect, by modelling the domain with truly oblique and not jagged microfin sides. Unfortunately improvement is only slight, suggesting that other issues still affect negatively the agreement. Among them, some concern the experimental part: it is difficult to let the drop fall exactly with the same height and shape of the simulations. The real drop detaches from a Plexiglas® block mimicking a infinite horizontal surface and in many cases it touches the base surface before complete detachment from the block (see the first frames of Figs. 16 and 17), being therefore different in shape from the spherical drop initialized in the simulations. The problem might be solved by slightly increasing the height of deposition, but this would influence a lot the final drop shape, which would become much more "flat" and "axisymmetric" with respect to the truly sessile one [26].

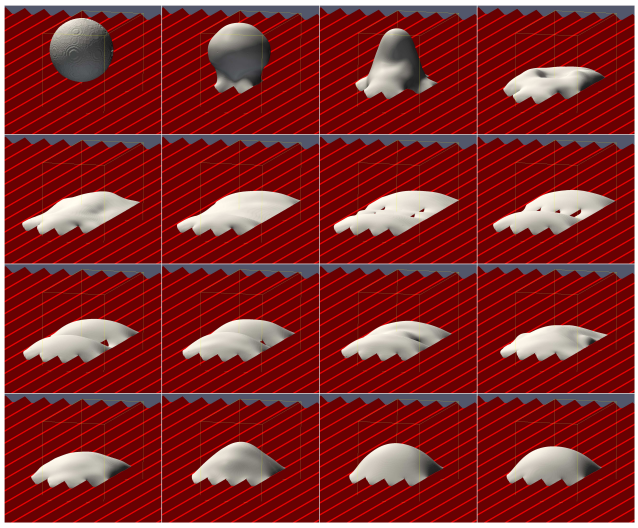

Figure 15: Drop deposition on the brass 400 μm microfin surface: 3D view of the numerical drop shape evolution (drop volume 80 · 10^{-9} m^3, time = 0:8:120 ms).

DROP-ONTO-DROP IMPACT

The last performed simulation concerned the impact of a drop onto another drop previously deposed on a flat hydrophilic surface. While a large number of studies can be found in literature concerning drop impact onto liquid films, from both the experimental and CFD points of view, very few papers [41] are available about drop-onto-drop impacts.
The simulation of this case started from the final results of the case of the wetting drop, with the latter in the role of the sessile drop. The second drop was initialized (again using the *funkySetFields* OpenFOAM® utility) as a sphere with diameter 2 mm, moving along the vertical direction at 1.4 m/s towards the domain floor and the first drop. Simulations were performed both using the *interFoam* solver and the *multiphaseInterFoam* (version 1.7.1) solver. With the latter, the water belonging to each drop can be distinguished during all the simulation [7]. Figure 21 shows the results: on the first column the *interFoam* output (where the colors indicate mesh resolution), on the second column the *multiphaseInterFoam* (where the colors indicate the different liquid phases, first and second drop). It can be noticed how the results are mesh independent and the agreement between the two-phase and the multiphase solvers is good for the first time steps, then the multiphase solver shows an evolution (including complex mixing between the two drops) which seems less realistic and credible. The third column of Fig. 21 shows experimental results. The resolution offered by the Nikon AW100 at high speed frame rates (320x240 px at 240 fps) was in this case insufficient to capture the details of the interaction between the two drops. Such results were therefore obtained by shooting photo sequences (at 4 fps, exposure time 1/4000 s) of many impacts with the D90 DSLR and extracting the most interesting images. Consequently, it is impossible to say at which precise time step the experimental pictures correspond, and only a qualitative comparison can be performed. Moreover, the drops dimensions do not strictly correspond to the numerical ones. Despite these heavy limitations, it may be said that the numerical simulations, particularly with the two-phase

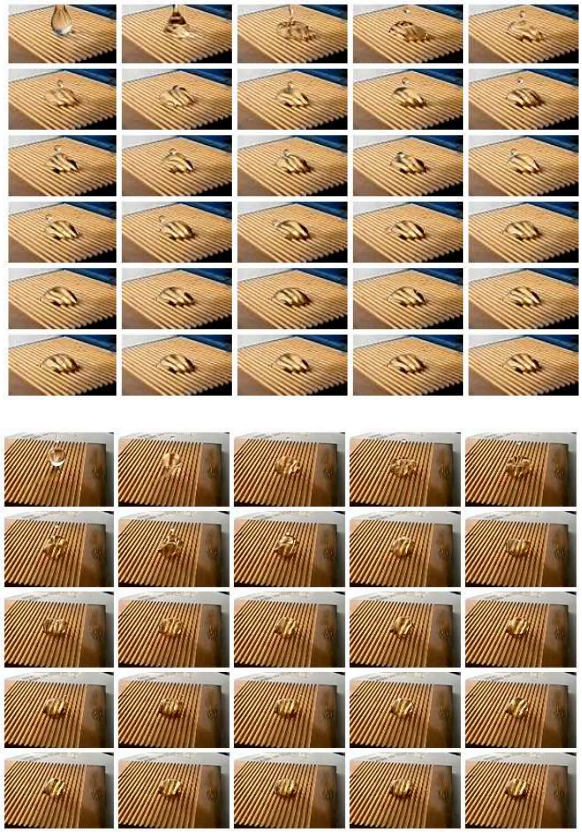

Figure 16: Drop deposition on the brass 400 µm microfin surface: experimental video acquisitions at 240 fps.

solver, correctly captured many phenomena observed during the experiments: e.g. the shape of the second drop just after the impact, the crater which forms in the first drop, the "donut" shape and central cone during the recoil.

CONCLUSIONS

Some comparisons were performed between numerical results, experimental results and models to evaluate the performances of the two-phase and multiphase solvers of the OpenFOAM® CFD package in the fields of drop deposition and low-speed impact. The cases of the sessile drop on a hydrophilic and hydrophobic flat and curved surfaces showed very good agreement between numerical results and experiments/models. Good qualitative agreement was also found for the cases of drop deposition on microfin surfaces and drop-onto-drop impact. From the quantitative point of view, the latter cases evidenced on the contrary some discrepancies, which may in part be attributable to modeling inaccuracies and difficulties in reproducing exactly the same initial conditions between simulations and experiments. In summary, the two-phase OpenFOAM® solver appears to be a fairly reliable tool for CFD simulations in the field of drop-surface interaction. Further validation is on the contrary needed for the multiphase solver, despite its very promising characteristics. Results can be obtained using a single personal computer, even if the simulation time for most cases is very long (between some days and one month).

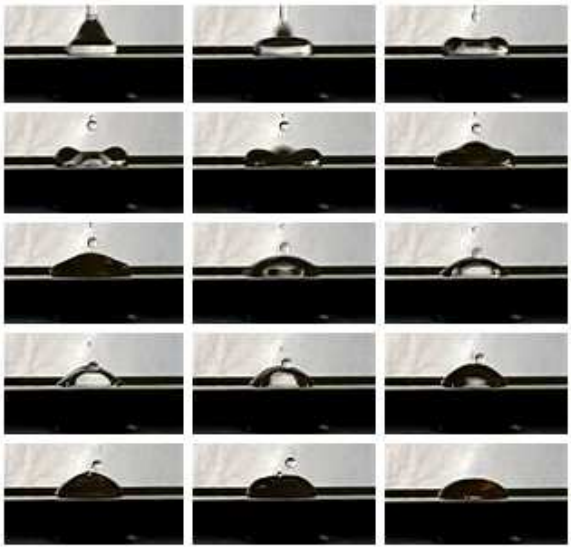

Figure 17: Drop deposition on the brass 400 µm microfin surface: experimental video acquisition at 240 fps, side view (fins are orthogonal to the camera direction).

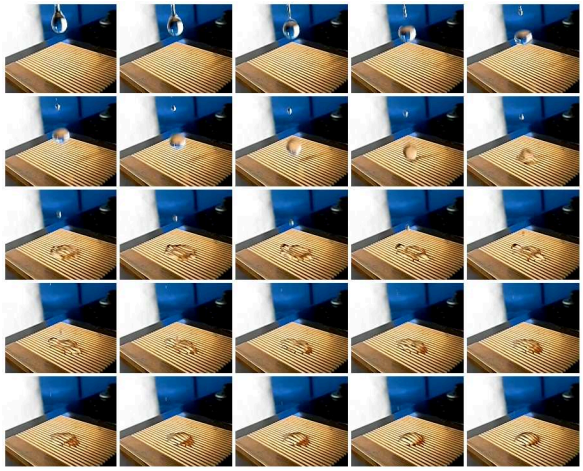

Figure 18: Low-speed impact onto the brass 400 µm microfin surface: experimental video acquisition at 240 fps.

ACKNOWLEDGMENTS

Prof. Giorgio Sotgia started the research activity about drop-surface interaction and microfin surfaces at the Department of Energy, Politecnico di Milano. His contribution is gratefully acknowledged.

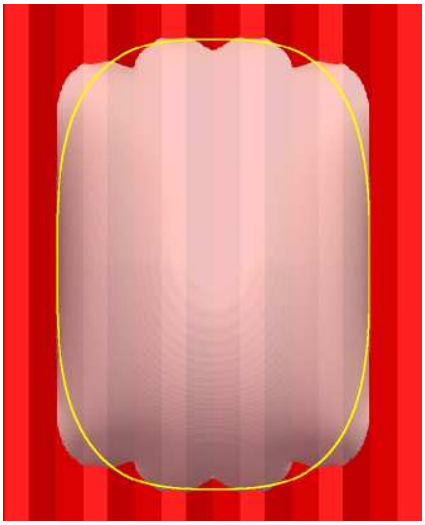

Figure 19: Deposition on the brass 400 µm microfin surface, 85 µl water drop: comparison of the simulated contact profile and apparent contact area (case 3a) with the model by Chen *et al.* [40].

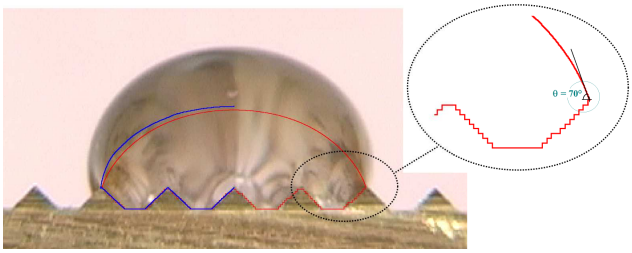

Figure 20: Deposition on the brass 400 µm microfin surface, 85 µl water drop: comparison of the simulated (red: case 3a, blue: case 3b) and experimental cross-section profile.

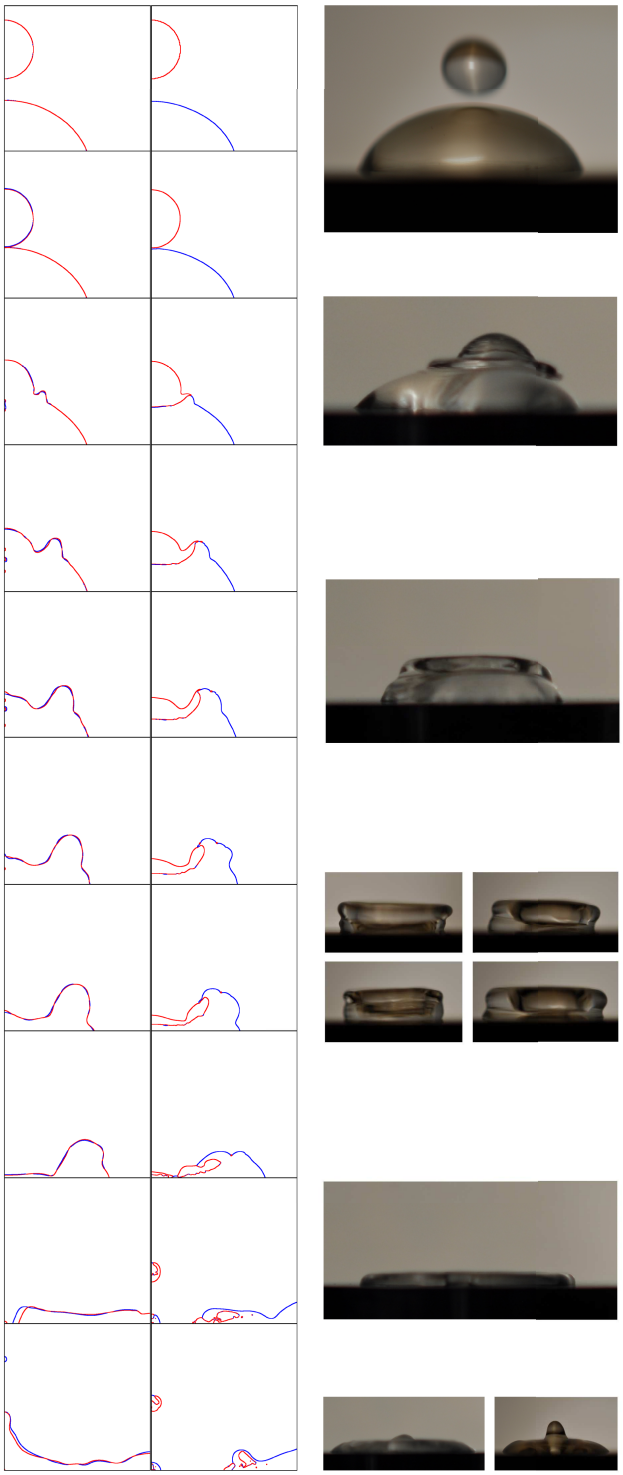

Figure 21: Drop-onto-drop impact simulated using *interFoam* (left column, blue: results with a mesh composed by 62500 cells, red: results with a mesh composed by 250000 cells) and *multiphaseInterFoam* (right column, blu: first drop, red: second drop), compared to experimental results (shots at 4 fps, exposure time 1/4000 s).

REFERENCES

[1] WS Atkins Consultants et al., *Best Practice Guidelines for Marine Applications of Computational Fluid Dynamics*, MarnetCFD, website: https://pronet.wsatkins.co.uk/marnet/publications/bpg.pdf, accessed June 2012.

[2] OpenFOAM®, The open source CFD toolbox, website: http://www.openfoam.com/, accessed March 2012.

[3] Costa A.B., Graham Cooks R., *Simulated splashes: Elucidating the mechanism of desorption electrospray ionization mass spectrometry*, Chemical Physics Letters, 2008, 464, 1-8.

[4] Berberovic E., van Hinsberg N.P., Jakirlic S., Roisman I.V., Tropea C., *Drop impact onto a liquid layer of finite thickness: Dynamics of the cavity evolution*, Physical Review E 79, 036306, 2009.

[5] Roisman I.V., Berberovic E., Jakirlic S., Tropea C., *Dynamics of two-phase flows induced by drop collisions*, Proceedings of the 7^{th} International Conference on Multiphase Flow (ICMF), Tampa (FL,USA), 2010.

[6] Fest-Santini S., Guilizzoni M., Santini M., Cossali G.E., *Drop impacts in pools: a comparison between high speed imaging and numerical simulations*, Proceedings of the Droplet Impact Phenomena & Spray Investigations (DIPSI) Workshop 2011, Dalmine (Italy).

[7] Santini M., Fest-Santini S., Guilizzoni M., Cossali G.E., *Drop impact onto a deep pool: study of the crater evolution*, Proceedings of the 24^{th} European Conference on Liquid Atomization and Spray Systems (ILASS - Europe 2011), Estoril (Portugal), 2011.

[8] E. Berberovic, *Investigation of Free-surface Flow Associated with Drop Impact: Numerical Simulations and Theoretical Modeling*, Ph.D. Thesis, TU Darmstadt, 2010.

[9] Roisman I.V., Weickgenannt C.M., Lembach A.N., Tropea C., *Drop impact close to a pore: experimental and numerical investigations*, Proceedings of the 23^{rd} Annual Conference on Liquid Atomization and Spray Systems, Brno, Czech Republic, September 2010.

[10] Sabry M.N., ElGharieb E., *Droplet dynamics over a super hydrophobic surface*, Thermal Issues in Emerging Technologies (ThETA 3), Cairo (Egypt), 2010.

[11] Gomaa H., Kumar S., Huber C., Weigand B., Peters B., *Numerical Comparison of 3D Jet Breakup Using a Compression Scheme and an Interface Reconstruction Based VOF-Code*, Proceedings of the 24^{th} European Conference on Liquid Atomization and Spray Systems (ILASS - Europe 2011), Estoril (Portugal), 2011.

[12] Jacobsen F., *Application of OpenFOAM for designing hydraulic water structures*, Open Source CFD International Conference, Barcelona (Spain), 2009.

[13] Paterson E., Smith K., Ford S., *Simulation Of Wakes, Wave Impact Loads, And Seakeeping Using OpenFOAM*, 4^{th} OpenFOAM Workshop, Montreal (Canada), 2009.

[14] Horvath A., Jordan C., Lukasser M., Kuttner C., Makaruk A., Harasek M., *CFD Simulation of Bubble Columns using the VOF Model: Comparison of commercial and Open Source Solvers with an Experiment*, Chemical Engineering Transactions, 2009, 18, 605-610.

[15] Gram A., *Modeling Free Surface Flow using multiphaseInterFoam*, PhD course in CFD with OpenSource software, Chalmers University of Technology, 2008, website: http://www.tfd.chalmers.se/~hani/kurser/OS_CFD_2008/AnnikaGram/reportAnnikaGram.pdf

[16] Weller H.G., Tabor G., Jasak H., Fureby C., *A tensorial approach to computational continuum mechanics using object-oriented techniques*, Computer in Physics, 1998, 12(6), 620-631.

[17] Jasak H., Weller H.G., *Interface-tracking capabilities of the InterGamma differencing scheme*, Technical Report, Imperial College of Science, Technology and Medicine, University of London, 1995.

[18] Gopala V.R., van Wachem B.G.M., *Volume of fluid methods for immiscible-fluid and free-surface flows*, Chemical Engineering Journal, 141 (2008) 204-221.

[19] Hirt, C.W., Nichols, B.D., *Volume of fluid (VOF) method for the dynamics of free boundaries*, Journal of Computational Physics, 1981, 39, 201-225.

[20] Brackbill J.U., Khote D.B, Zemach C., *A Continuum Method for Modeling Surface Tension*, Journal of Computational Physics, 1992, 100, 335-354.

[21] Ferziger J.H., Peric M., *Computational Methods for Fluid Dynamics*, 3^{rd} ed., Springer, 2002.

[22] Andersson P., *Tutorial multiphaseInterFoam for the damBreak4phase case*, PhD course in CFD with OpenSource software, Chalmers University of Technology, 2010, website: http://www.tfd.chalmers.se/~hani/kurser/OS_CFD_2010/patrikAndersson/patrikAnderssonReport.pdf

[23] Roisman I.V., Opfer L., Tropea C., Raessi M., Mostaghimi J., Chandra S., *Drop impact onto a dry surface: Role of the dynamic contact angle*, Colloids and Surfaces A: Physicochemical and Engineering Aspects, 2008, 322, 183-191.

[24] Criscione A., Rohrig R., Jakirlic S., Roisman I.V., Tropea C., *Impacting Droplets: Dynamic Contact Angle Modeling in OpenFOAM*, 7^{th} OpenFOAM Workshop, Darmstadt (Germany), 2012.

[25] Guilizzoni M., *Drop shape visualization and contact angle measurement on curved surfaces*, Journal of Colloid and Interface Science, 2011, 364, 230-236.

[26] Guilizzoni M., Sotgia G., *Experimental analysis on the shape and evaporation of water drops on high effusivity, microfinned surfaces*, Experimental Thermal and Fluid Science, 2010, 34, 93-103.

[27] Rotenberg Y., Boruvka L., Neumann A.W., *Determination of surface tension and contact angle from the shapes of axisymmetric fluid interfaces*, Journal of Colloid and Interface Science, 1983, 93(1), 169-183.

[28] Fest-Santini S., Guilizzoni M., Santini M., Cossali G.E., *Drop Impact onto hydrophobic and superhydrophobic surfaces*, XXIX National UIT Heat Transfer Conference, Turin (Italy), 2011.

[29] Hu, H., Larson, G., *Evaporation of a sessile droplet on a substrate*, Journal of Physical Chemistry, 2002, 106, 1334-1344.

[30] Ruiz O.E., Black W.Z., *Evaporation of water droplets placed on a heated horizontal surface*, Journal of Heat Transfer - Transactions of the ASME, 2002, 24, 854-863.

[31] Mollaret R., Sefiane K., Christy J.R.E., Veyret D., *Experimental and Numerical Investigation of the Evaporation into Air of a Drop on a Heated Surface*, Chemical Engineering Research and Design, 2004, 82(4), 471-480.

[32] Cho S.C., Wang Y., Chen K.S., *Droplet dynamics in a polymer electrolyte fuel cell gas flow channel: Forces, deformation, and detachment. I: Theoretical and numerical analyses*, Journal of Power Sources, 2012, 206, 119-128.

[33] Zhu X., Sui P.C., Djilali N., *Dynamic behaviour of liquid water emerging from a GDL pore into a PEMFC gas flow channel*, Journal of Power Sources, 2007, 172, 287-295.

[34] Zhu X., Liao Q., Sui P.C., Djilali N., *Numerical investigation of water droplet dynamics in a low-temperature fuel cell microchannel: Effect of channel geometry*, Journal of Power Sources, 2010, 195, 801-812.

[35] Bormashenko E., *Wetting of Flat and Rough Curved Surfaces*, Journal of Physical Chememistry C, 2009, 113, 17275-17277.

[36] Tadmor R., Yadav P.S., *As-placed contact angles for sessile drops*, Journal of Colloid and Interface Science, 2008, 317, 241-246.

[37] Extrand C.W., Moon S.I., *Contact Angles on Spherical Surfaces*, Langmuir, 2008, 24, 9470-9473.

[38] Guilizzoni M., Sotgia G., Osnato F., *Evaporation of sessile and impinging water drops on microfinned metallic surfaces*, XXVII National UIT Heat Transfer Conference, Reggio Emilia (Italy), 2009.

[39] Kannan R., Sivakumar D., *Drop impact process on a hydrophobic grooved surface*, Colloids and Surfaces A: Physicochem. Eng. Aspects 2008, 317, 694-704.

[40] Sommers A.D., Jacobi A.M., *Wetting phenomena on micro-grooved aluminum surfaces and modeling of the critical droplet size*, Journal of Colloid and Interface Science, 2008, 328, 402-411.

[41] Nikolopoulos N., Strotos G., Nikas K.S.P., Theodorakakos A., Gavaises M., Marengo M., Cossali G.E., *Single droplet impacts onto deposited drops. Numerical analysis and comparison*, Atomization and Sprays, 2010, 20 (11), 935-953.